Journal of Sound and Vibration (1999) **224**(4), 709–732
Article No. jsvi.1999.2209, available online at http://www.idealibrary.com on IDEAL®

DYNAMICS OF A CONCENTRICALLY OR ECCENTRICALLY SUBMERGED CIRCULAR CYLINDRICAL SHELL IN A FLUID-FILLED CONTAINER

KYEONG-HOON JEONG

Korea Atomic Energy Research Institute, P. O. Box 105, *Yusong, Taejon* 305-600, *Korea*

(*Received* 29 *October* 1998, *and in final form* 27 *January* 1999)

A theoretical study is presented on the natural frequencies of a circular cylindrical shell concentrically or eccentrically submerged in a fluid-filled rigid cylindrical container. In this analysis, it is assumed that the shell is clamped at both ends, and an annulus between the shell and the rigid container is filled with a non-viscous and compressible fluid. The velocity potential for fluid motion is formulated in terms of Fourier series expansion, and the modal displacements of the shell are expanded with the finite Fourier series using the finite Fourier transformation. Along the contacting surface between the shell and fluid, the compatibility requirement is applied for fluid–structure interaction. In order to consider eccentricity between the axes of the shell and the container, an additional shifted co-ordinate system is introduced. Graf's additional theorem and Beltrami's theorem are used for the translated forms of the Bessel functions in the shifted co-ordinate system. The proposed analytical method for the concentrically submerged shell is verified by observing an excellent agreement with the finite-element analysis results. In order to evaluate the dynamic characteristics of the fluid-coupled system, the effects of annular fluid gap and eccentricity of the shell on the natural frequencies are investigated. © 1999 Academic Press

1. INTRODUCTION

The free vibration characteristics of a fluid-surrounded cylindrical shell subjected to various loads have been of great concern in engineering design. Hence, many investigations in this area have been carried out. The free vibration analysis of two infinitely long, coaxial cylinders containing fluid was performed by Krajcinovic [1]. Chen and Rosenberg [2] derived a frequency equation for two concentrically arranged circular cylindrical shells containing and separated by incompressible fluid and obtained an approximate closed-form solution. Au-Yang [3] treated the internal structure of a pressurized water reactor as a system of finite coaxial cylinders immersed in a fluid. He estimated the virtual mass and coupling coefficient of two finite cylinders with different lengths immersed in fluid for the simply supported boundary condition. The free vibration of an infinitely long cylindrical shell under axisymmetrical hydrodynamic pressures of the external and

0022-460X/99/290709 + 24 $30.00/0 © 1999 Academic Press

internal fluids was studied using Fourier cosine transformation by Endo and Tosaka [4]. Tani et al. [5] performed a study on the free vibration of clamped coaxial cylindrical shells partially filled with incompressible and inviscid fluid. The theoretical analysis was based upon the Galerkin method and the velocity potential theory for the fluid. The vibrational characteristic of two concentric submerged cylindrical shells coupled by entrained fluid was studied by Yoshigawa et al. [6]. Chiba [7] carried out a theoretical and experimental study on the free vibration of clamped–free cylindrical shell, which is partially and concentrically submerged in a liquid-filled container using the Galerkin method. Jeong and Lee [8] suggested a theoretical method to study the free vibration of a liquid-surrounded cylindrical shell. Recently Chiba and Osumi [9] carried out a theoretical and experimental study on the free vibration of a clamped–clamped cylindrical shell which is partially filled with liquid and, at the same time, partially submerged in a liquid. A theoretical method to study the free vibration of coaxial cylindrical shells coupled with compressible fluid was suggested and the presence of some mixed vibrational modes was found by Jeong [10]. Danila et al. [11] suggested a calculating method of the scattered field due to a plane wave incident on one or several cylindrical fluid–fluid interfaces using the generalized Debye series expansion. The theoretical method is applied to a concentric and a non-concentric fluid shell and then extended to the multi-layered cylindrical structure.

However, few theoretical studies have been made on the free vibration of a circular cylindrical shell submerged in a compressible fluid-filled cylindrical container. Therefore, this paper attempts to develop an analytical method that calculates the natural frequencies of a cylindrical shell concentrically or eccentrically submerged in a fluid-filled cylindrical container using the series expansion methods. The clamped boundary condition was assumed for both ends of the shell. However, the theory can be extended to any arbitrary classical boundary conditions using an additional simple formulation. This analytical method for the concentrically submerged case was verified by finite-element modelling (FEM).

2. THEORETICAL BACKGROUND

2.1. EQUATION OF MOTION AND BOUNDARY CONDITIONS OF A CIRCULAR CYLINDRICAL SHELL

Consider a circular cylindrical shell with a clamped boundary condition at both ends, as illustrated in Figure 1. The shell can be concentrically or eccentrically submerged in a fluid-filled container. The cylindrical shell has mean radius R, height L, and wall thickness h. The Sanders' shell equations [8, 10] as the governing equations for the shell where the hydrodynamic effect is considered, can be written as

$$R^2 u_{,xx} + \frac{(1-\mu)}{2}\left(1+\frac{k}{4}\right)u_{,\theta\theta} + R\left\{\frac{(1-\mu)}{2} - \frac{3(1-\mu)}{8}k\right\}v_{,x\theta} + \mu R w_{,x} + \frac{(1-\mu)}{2}Rk w_{,x\theta\theta} = \gamma^2 u_{,tt}, \tag{1a}$$

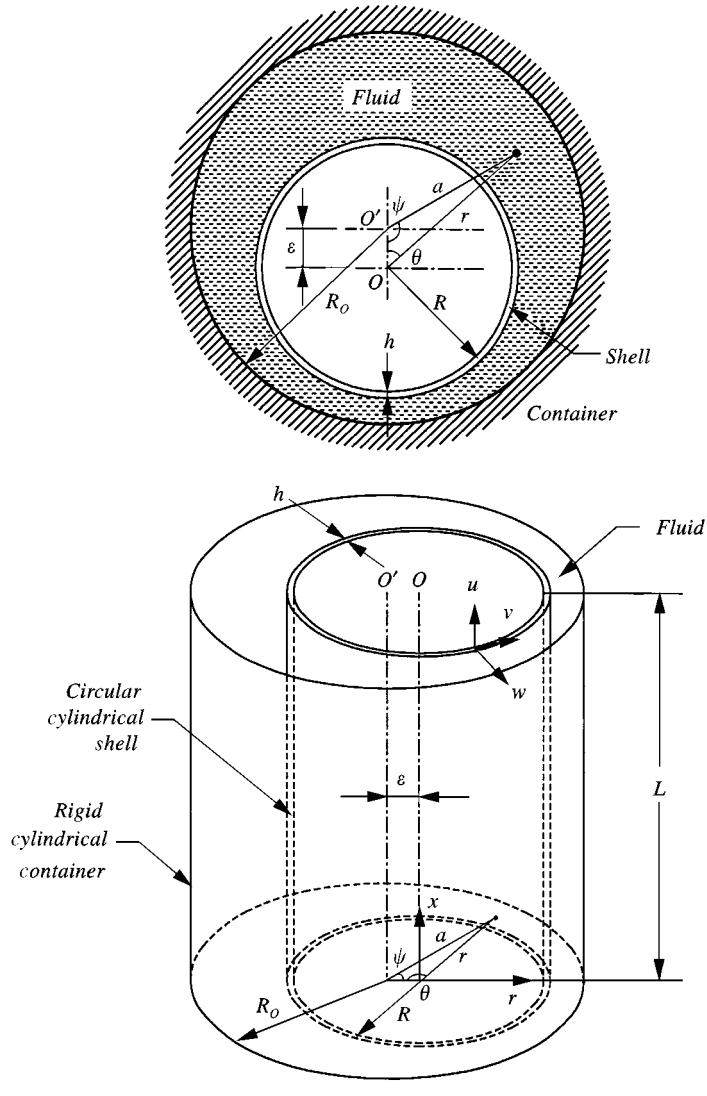

Figure 1. An eccentrically submerged cylindrical shell in a fluid-filled rigid container.

$$R\left\{\frac{(1-\mu)}{2}-\frac{3(1-\mu)}{8}k\right\}u_{,x\theta}+(1+k)v_{,\theta\theta}+\frac{(1-\mu)}{2}R^2\left(1+\frac{9k}{4}\right)v_{,xx}$$

$$-\frac{(3-\mu)}{2}R^2kw_{,xx\theta}+w_{,\theta}-kw_{,\theta\theta\theta}=\gamma^2v_{,tt}, \tag{1b}$$

$$\frac{(1-\mu)}{2}Rku_{,x\theta\theta}+\mu Ru_{,x}-\frac{(3-k)}{2}R^2kv_{,xx\theta}+v_{,\theta}+w+k(R^4w_{,xxx}+2R^2w_{,xx\theta\theta}$$

$$+w_{,\theta\theta\theta\theta}-v_{,\theta\theta\theta})=-\gamma^2u_{,tt}+\frac{R^2p}{D}. \tag{1c}$$

The comma in the equations denotes a partial derivative with respect to the corresponding variable. For a complete description of the shell motions, it is necessary to add boundary conditions to the equations of motion. Consider the simplest end arrangements of the shell on the top and bottom supports. At both ends of a concentrically or eccentrically arranged shell with respect to a rigid circular cylindrical container, all the boundary conditions will obviously hold for the case of sine–cosine–cosine (SCC) formulation [12]:

$$M_x(0) = N_x(0) = v(0) = w(0) = 0 \quad \text{for the bottom support of the shell,} \tag{2a}$$

$$M_x(L) = N_x(L) = v(L) = w(L) = 0 \quad \text{for the top support of the shell} \tag{2b}$$

where M_x and N_x denote the bending moment and the membrane tensile force respectively. All geometric boundary conditions applicable to the clamped–clamped shell can be reduced to the following equations for the ends of the shell [13]:

$$v(0) = w(0) = v(L) = w(L) = 0. \tag{3}$$

The relationships between the boundary forces and displcements are

$$N_x = D\left[u_{,x} + \frac{\mu}{R}v_{,\theta} + \frac{\mu}{R}w\right], \tag{4a}$$

$$N_{x\theta} = \frac{D(1-\mu)}{2}\left[\frac{1}{R}\left(1 - \frac{3}{4}k\right)u_{,\theta} + \left(1 + \frac{9}{4}k\right)v_{,x} - 3kw_{,x\theta}\right], \tag{4b}$$

$$Q_x = K\left[-\frac{(1-\mu)}{2R^3}u_{,\theta\theta} + \frac{(3-\mu)}{2R^2}v_{,x\theta} - \frac{(2-\mu)}{R^2}w_{,x\theta\theta} - w_{,xxx}\right], \tag{4c}$$

$$M_x = K\left[\frac{\mu}{R^2}(v_{,\theta} - w_{,\theta\theta}) - w_{,xx}\right]; \tag{4d}$$

where $D = Eh/(1-\mu^2)$, $K = Eh^3/12(1-\mu^2)$, $k = h^2/12R^2$. $N_{x\theta}$ and Q_x denote the membrane shear force and transverse shear force per unit length, respectively.

2.2. MODAL FUNCTIONS

A general relation for the dynamic displacements in any vibration mode of the shell can be written in the following form for the cylindrical co-ordinate r, θ;

$$u(x, \theta, t) = u(x, \theta)\exp(\mathrm{i}\omega t), \tag{5a}$$

$$v(x, \theta, t) = v(x, \theta)\exp(\mathrm{i}\omega t), \tag{5b}$$

$$w(x, \theta, t) = w(x, \theta)\exp(\mathrm{i}\omega t), \tag{5c}$$

where $u(x, \theta)$, $v(x, \theta)$, and $w(x, \theta)$ are modal functions corresponding to the axial, tangential, and radial displacements for the shell respectively. These modal functions along the axial direction can be described by a sum of linear combinations of the Fourier series that are orthogonal:

$$u(x, \theta) = \sum_{n=1}^{\infty} \sum_{s=1}^{\infty} A_{sn} \sin\left(\frac{s\pi x}{L}\right) \cos n\theta, \tag{6a}$$

$$v(x, \theta) = \sum_{n=1}^{\infty} \left[B_{on} + \sum_{s=1}^{\infty} B_{sn} \cos\left(\frac{s\pi x}{L}\right) \right] \sin n\theta, \tag{6b}$$

$$w(x, \theta) = \sum_{n=1}^{\infty} \left[C_{on} + \sum_{s=1}^{\infty} C_{sn} \cos\left(\frac{s\pi x}{L}\right) \right] \cos n\theta. \tag{6c}$$

The derivatives of the above modal functions for the shell can be obtained using the finite Fourier transformation [13, 14]. The modal functions and their derivatives of the cylindrical shell were described in reference [13].

2.3. EQUATION OF FLUID MOTION

The inviscid, irrotational and compressible fluid movement due to shell vibration is described by the Helmholz equation

$$\Phi_{,rr} + \frac{1}{r}\Phi_{,r} + \frac{1}{r^2}\Phi_{,\theta\theta} + \Phi_{,xx} = \frac{1}{c^2}\Phi_{,tt}, \tag{7}$$

where c is the speed of sound in the fluid medium equal to $\sqrt{B/\rho_o}$, B is the bulk modulus of elasticity of fluid and ρ_o stands for the fluid density. It is possible to separate the function Φ with respect to x by observing that, in the axial direction, the rigid surfaces support the edges of the shell; thus,

$$\Phi(x, r, \theta, t) = \mathrm{i}\omega\phi(r, \theta, x)\exp(\mathrm{i}\omega t) = \mathrm{i}\omega\eta(r, \theta) f(x)\exp(\mathrm{i}\omega t), \tag{8}$$

where ω is the fluid-coupled frequency of the shell. Substitution of equation (8) into the partial differential equation (7) gives

$$\frac{\eta(r, \theta)_{,rr} + (1/r)\eta(r, \theta)_{,r} + (1/r^2)\eta(r, \theta)_{,\theta\theta} + (\omega/c)^2\eta(r, \theta)}{\eta(r, \theta)} = -\frac{f(x)_{,xx}}{f(x)} = \left(\frac{s\pi}{L}\right)^2. \tag{9}$$

It is possible to solve the partial differential equation (9) by the separation of the variables. The solution can be obtained with respect to the original cylindrical

co-ordinates, r, θ and x:

$$\phi(r,\theta,x)=\sum_{n=1}^{\infty}\left[\begin{array}{l} D_{on}\mathrm{J}_n\left(\dfrac{\omega r}{c}\right)+F_{on}\mathrm{Y}_n\left(\dfrac{\omega r}{c}\right) \\ \quad +\displaystyle\sum_{s=1}^{\infty}\{D_{sn}\mathrm{I}_n(\alpha_{sn}r)+F_{sn}\mathrm{K}_n(\alpha_{sn}r)\}\cos\left(\frac{s\pi x}{L}\right)\end{array}\right]\cos n\theta$$

$$\text{for } \frac{s\pi}{L}\geqslant\frac{\omega}{c}, \tag{10a}$$

$$\phi(r,\theta,x)=\sum_{n=1}^{\infty}\left[\begin{array}{l} D_{on}\mathrm{J}_n\left(\dfrac{\omega r}{c}\right)+F_{on}\mathrm{Y}_n\left(\dfrac{\omega r}{c}\right) \\ \quad +\displaystyle\sum_{s=1}^{\infty}\{D_{sn}\mathrm{J}_n(\alpha_{sn}r)+F_{sn}\mathrm{Y}_n(\alpha_{sn}r)\}\cos\left(\frac{s\pi x}{L}\right)\end{array}\right]\cos n\theta$$

$$\text{for } \frac{s\pi}{L}<\frac{\omega}{c}, \tag{10b}$$

where J_n and Y_n are Bessel functions of the first and second kinds of order n, whereas I_n and K_n are modified Bessel functions of the first and second kinds of order n, ϕ is the spatial velocity potential of the contained compressible fluid, and α_{sn} is related to the speed of sound in the fluid medium,

$$\alpha_{sn}=\sqrt{\left|\left(\frac{s\pi}{L}\right)^2-\left(\frac{\omega}{c}\right)^2\right|}\quad \text{for } s=1,2,3,\ldots. \tag{11}$$

Equations (10a) and (10b) automatically satisfy by boundary conditions that appear as follows: (a) impermeable rigid surface on the bottom is

$$\frac{\partial\phi(r,\theta,x)}{\partial x}=0\quad \text{at } x=0; \tag{12}$$

(b) as there exists no free surface, the axial fluid velocity at the rigid top is also zero, so

$$\frac{\partial\phi(r,\theta,x)}{\partial x}=0\quad \text{at } x=L. \tag{13}$$

2.4. GENERAL FORMULATION FOR CONCENTRICALLY SUBMERGED SHELL

When the shell is concentrically submerged in the fluid-filled container, the radial fluid velocity along the outer wetted surface of the shell must be identical to the

radial velocity of a flexible shell, so

$$\frac{\partial\phi(r,\theta,x)}{\partial r} = -w(x,\theta) \quad \text{at } r = R. \tag{14}$$

Additionally, the radial fluid velocity along the wetted surface of the outer rigid container must be zero, and so

$$\frac{\partial\phi(r,\theta,x)}{\partial r} = 0 \quad \text{at } r = R_o. \tag{15}$$

Substitution of equations (6c), (10a) and (10b) into equations (14) and (15) gives the following relationships:

$$\sum_{n=1}^{\infty}\left[\left(\frac{\omega}{c}\right)\left\{D_{on}\mathrm{J}'_n\left(\frac{\omega R}{c}\right) + F_{on}\mathrm{Y}'_n\left(\frac{\omega R}{c}\right)\right\} + \sum_{s=1}^{\infty}\alpha_{sn}\{D_{sn}\mathrm{I}'_n(\alpha_{sn}R) + F_{sn}\mathrm{K}'_n(\alpha_{sn}R)\}\cos\left(\frac{s\pi x}{L}\right)\right]\cos n\theta$$

$$= -\sum_{n=1}^{\infty}\left[C_{on} + \sum_{s=1}^{\infty}C_{sn}\cos\left(\frac{s\pi x}{L}\right)\right]\cos n\theta \quad \text{for } \frac{s\pi}{L} \geqslant \frac{\omega}{c}, \tag{16a}$$

$$\sum_{n=1}^{\infty}\left[\left(\frac{\omega}{c}\right)\left\{D_{on}\mathrm{J}'_n\left(\frac{\omega R}{c}\right) + F_{on}\mathrm{Y}'_n\left(\frac{\omega R}{c}\right)\right\} + \sum_{s=1}^{\infty}\alpha_{sn}\{D_{sn}\mathrm{J}'_n(\alpha_{sn}R) + F_{sn}\mathrm{Y}'_n(\alpha_{sn}R)\}\cos\left(\frac{s\pi x}{L}\right)\right]\cos n\theta$$

$$= -\sum_{n=1}^{\infty}\left[C_{on} + \sum_{s=1}^{\infty}C_{sn}\cos\left(\frac{s\pi x}{L}\right)\right]\cos n\theta \quad \text{for } \frac{s\pi}{L} < \frac{\omega}{c}, \tag{16b}$$

$$\left(\frac{\omega}{c}\right)\left\{D_{on}\mathrm{J}'_n\left(\frac{\omega R_o}{c}\right) + F_{on}\mathrm{Y}'_n\left(\frac{\omega R_o}{c}\right)\right\} + \sum_{s=1}^{\infty}\alpha_{sn}\{D_{sn}\mathrm{I}'_n(\alpha_{sn}R_o) + F_{sn}\mathrm{K}'_n(\alpha_{sn}R_o)\}\cos\left(\frac{s\pi x}{L}\right) = 0$$

$$\text{for } \frac{s\pi}{L} \geqslant \frac{\omega}{c}, \tag{16c}$$

$$\left(\frac{\omega}{c}\right)\left\{D_{on}\mathrm{J}'_n\left(\frac{\omega R_o}{c}\right) + F_{on}\mathrm{Y}'_n\left(\frac{\omega R_o}{c}\right)\right\} + \sum_{s=1}^{\infty}\alpha_{sn}\{D_{sn}\mathrm{J}'_n(\alpha_{sn}R_o) + F_{sn}\mathrm{Y}'_n(\alpha_{sn}R_o)\}\cos\left(\frac{s\pi x}{L}\right) = 0$$

$$\text{for } \frac{s\pi}{L} < \frac{\omega}{c}, \tag{16d}$$

Now, all unknown coefficients D_{on}, F_{on}, D_{sn} and F_{sn} related to the fluid motion will be written in terms of the coefficients C_{on} and C_{sn} related to the shell motion:

$$D_{on} = \frac{\mathrm{Y}'_n(\omega R_o/c)}{(\omega/c)[\mathrm{J}'_n(\omega R_o/c)\mathrm{Y}'_n(\omega R/c) - \mathrm{J}'_n(\omega R/c)\mathrm{Y}'_n(\omega R_o/c)]} C_{on}, \tag{17a}$$

$$F_{on} = \frac{\mathrm{J}'_n(\omega R_o/c)}{(\omega/c)[\mathrm{J}'_n(\omega R/c)\mathrm{Y}'_n(\omega R_o/c) - \mathrm{J}'_n(\omega R_o/c)\mathrm{Y}'_n(\omega R/c)]} C_{on}, \tag{17b}$$

$$D_{sn} = \frac{\mathrm{K}'_n(\alpha_{sn} R_o)}{(\alpha_{sn})[\mathrm{I}'_n(\alpha_{sn} R_o)\mathrm{K}'_n(\alpha_{sn} R) - \mathrm{I}'_n(\alpha_{sn} R)\mathrm{K}'_n(\alpha_{sn} R_o)]} C_{sn} \quad \text{for } \frac{s\pi}{L} \geqslant \frac{\omega}{c}, \tag{17c}$$

$$D_{sn} = \frac{\mathrm{Y}'_n(\alpha_{sn} R_o)}{(\alpha_{sn})[\mathrm{J}'_n(\alpha_{sn} R_o)\mathrm{Y}'_n(\alpha_{sn} R) - \mathrm{J}'_n(\alpha_{sn} R)\mathrm{Y}'_n(\alpha_{sn} R_o)]} C_{sn} \quad \text{for } \frac{s\pi}{L} < \frac{\omega}{c}, \tag{17d}$$

$$F_{sn} = \frac{\mathrm{I}'_n(\alpha_{sn} R_o)}{(\alpha_{sn})[\mathrm{I}'_n(\alpha_{sn} R)\mathrm{K}'_n(\alpha_{sn} R_o) - \mathrm{I}'_n(\alpha_{sn} R_o)\mathrm{K}'_n(\alpha_{sn} R)]} C_{sn} \quad \text{for } \frac{s\pi}{L} \geqslant \frac{\omega}{c}, \tag{17e}$$

$$F_{sn} = \frac{\mathrm{J}'_n(\alpha_{sn} R_o)}{(\alpha_{sn})[\mathrm{J}'_n(\alpha_{sn} R)\mathrm{Y}'_n(\alpha_{sn} R_o) - \mathrm{J}'_n(\alpha_{sn} R_o)\mathrm{Y}'_n(\alpha_{sn} R)]} C_{sn} \quad \text{for } \frac{s\pi}{L} < \frac{\omega}{c}. \tag{17f}$$

2.5. GENERAL FORMULATION FOR ECCENTRICALLY SUBMERGED SHELL

On the other hand, for the eccentrically submerged shell, the velocity potential of equations (10a) and (10b) can be transformed into the shifted cylindrical co-ordinates, (a, ψ, x) by Graf's addition theorem and Beltrami's theorem [15]:

$$\phi(a, \psi, x) =$$

$$\sum_{n=1}^{\infty} \sum_{m=-\infty}^{\infty} \left[\begin{array}{l} \left\{ D_{on} \mathrm{J}_{n+m}\left(\frac{\omega a}{c}\right) + F_{on} \mathrm{Y}_{n+m}\left(\frac{\omega a}{c}\right) \right\} \mathrm{J}_m\left(\frac{\omega \varepsilon}{c}\right) \\ + \sum_{s=1}^{\infty} \{ D_{sn}(-1)^m \mathrm{I}_{n+m}(\alpha_{sn} a) + F_{sn} \mathrm{K}_{n+m}(\alpha_{sn} a) \} \mathrm{I}_m(\alpha_{sn} \varepsilon) \cos\left(\frac{s\pi x}{L}\right) \end{array} \right] \cos m\psi$$

$$\text{for } \frac{s\pi}{L} \geqslant \frac{\omega}{c}, \tag{18a}$$

$$\phi(a, \psi, x) =$$

$$\sum_{n=1}^{\infty} \sum_{m=-\infty}^{\infty} \left[\begin{array}{l} \left\{ D_{on} \mathrm{J}_{n+m}\left(\frac{\omega a}{c}\right) + F_{on} \mathrm{Y}_{n+m}\left(\frac{\omega a}{c}\right) \right\} \mathrm{J}_m\left(\frac{\omega \varepsilon}{c}\right) \\ + \sum_{s=1}^{\infty} \{ D_{sn} \mathrm{J}_{n+m}(\alpha_{sn} a) + F_{sn} \mathrm{Y}_{n+m}(\alpha_{sn} a) \} \mathrm{J}_m(\alpha_{sn} \varepsilon) \cos\left(\frac{s\pi x}{L}\right) \end{array} \right] \cos m\psi$$

$$\text{for } \frac{s\pi}{L} < \frac{\omega}{c}. \tag{18b}$$

It is convenient to handle the boundary condition along the surface of the rigid container when the velocity potential is transformed from the origin "O" into the shifted origin "O'". The radial fluid velocity along the outer wetted surface of the shell must be identical to that of the flexible shell. Therefore, equations (16c) and (16d) should be satisfied, and the radial fluid velocity along the wetted surface of the outer rigid container that maintains eccentricity to the shell must be zero. Hence

$$\frac{\partial \phi(x, \psi, a)}{\partial a} = 0 \quad \text{at } a = R_o. \tag{19}$$

Substitution of equations (6c), (18a) and (18b) into equations (14) ad (19) gives equation (16a, b) and the relationships

$$\sum_{m=-\infty}^{\infty} \left[\left(\frac{\omega}{c}\right) \mathrm{J}_m\left(\frac{\omega\varepsilon}{c}\right) \left\{ D_{on} \mathrm{J}'_{n+m}\left(\frac{\omega R_o}{c}\right) + F_{on} \mathrm{Y}'_{n+m}\left(\frac{\omega R_o}{c}\right) \right\} + \sum_{s=1}^{\infty} \alpha_{sn} \mathrm{I}_m(\alpha_{sn}\varepsilon) \{ D_{sn}(-1)^m \mathrm{I}'_{n+m}(\alpha_{sn} R_o) + F_{sn} \mathrm{K}'_{n+m}(\alpha_{sn} R_o) \} \cos\left(\frac{s\pi x}{L}\right) \right] = 0$$

$$\text{for } \frac{s\pi}{L} \geqslant \frac{\omega}{c}, \tag{20a}$$

$$\sum_{m=-\infty}^{\infty} \left[\left(\frac{\omega}{c}\right) \mathrm{J}_m\left(\frac{\omega\varepsilon}{c}\right) \left\{ D_{on} \mathrm{J}'_{n+m}\left(\frac{\omega R_o}{c}\right) + F_{on} \mathrm{Y}'_{n+m}\left(\frac{\omega R_o}{c}\right) \right\} + \sum_{s=1}^{\infty} \alpha_{sn} \mathrm{J}_m(\alpha_{sn}\varepsilon) \{ D_{sn} \mathrm{J}'_{n+m}(\alpha_{sn} R_o) + F_{sn} \mathrm{Y}'_{n+m}(\alpha_{sn} R_o) \} \cos\left(\frac{s\pi x}{L}\right) \right] = 0$$

$$\text{for } \frac{s\pi}{L} < \frac{\omega}{c}. \tag{20b}$$

Now, all unknown coefficients D_{on}, F_{on}, D_{sn} and F_{sn} related to the fluid motion will be written in terms of the coefficients C_{on} and C_{sn} related to the shell motion using equations (16a, b) and (20a, b).

$$F_{on} = W_{n1} D_{on}, \quad D_{on} = \Gamma_{n1} C_{on}, \quad F_{on} = \Gamma_{n2} C_{on}: \tag{21a–c}$$

For $\frac{s\pi}{L} \geqslant \frac{\omega}{c}$,

$$F_{sn} = W_{n2} D_{sn}, \quad D_{sn} = \Gamma_{sn3} C_{sn}, \quad F_{sn} = \Gamma_{sn5} C_{sn}: \tag{21d–f}$$

For $\frac{s\pi}{L} < \frac{\omega}{c}$,

$$F_{sn} = W_{n3} D_{sn}, \quad D_{sn} = \Gamma_{sn4} C_{sn}, \quad F_{sn} = \Gamma_{sn6} C_{sn}: \tag{21g–i}$$

where

$$W_{n1} = -\frac{\sum_{m=-\infty}^{\infty} \{J_m(\omega\varepsilon/c) J'_{n+m}(\omega R_o/c)\}}{\sum_{m=-\infty}^{\infty} \{J_m(\omega\varepsilon/c) Y'_{n+m}(\omega R_o/c)\}}, \tag{22a}$$

$$W_{n2} = -\frac{\sum_{m=-\infty}^{\infty} \{I_m(\alpha_{sn}\varepsilon)(-1)^m I'_{n+m}(\alpha_{sn} R_o)\}}{\sum_{m=-\infty}^{\infty} \{I_m(\alpha_{sn}\varepsilon) K'_{n+m}(\alpha_{sn} R_o)\}}, \tag{22b}$$

$$W_{n3} = -\frac{\sum_{m=-\infty}^{\infty} \{J_m(\alpha_{sn}\varepsilon) J'_{n+m}(\alpha_{sn} R_o)\}}{\sum_{m=-\infty}^{\infty} \{J'_m(\alpha_{sn}\varepsilon) Y'_{n+m}(\alpha_{sn} R_o)\}}, \tag{22c}$$

$$\Gamma_{n1} = -\left(\frac{c}{\omega}\right)\left[J'_n\left(\frac{\omega R}{c}\right) + W_{n1} Y'_n\left(\frac{\omega R}{c}\right)\right]^{-1}, \tag{22d}$$

$$\Gamma_{n2} = W_{n1}\Gamma_{n1}, \quad \Gamma_{sn3} = \frac{-1}{\alpha_{sn}[I'_n(\alpha_{sn}R) + W_{n2} K'_n(\alpha_{sn}R)]}, \tag{22e, f}$$

$$\Gamma_{sn4} = \frac{-1}{\alpha_{sn}[J'_n(\alpha_{sn}R) + W_{n3} Y'_n(\alpha_{sn}R)]}, \quad \Gamma_{sn5} = W_{n2}\Gamma_{sn3}, \quad \Gamma_{sn6} = W_{n3}\Gamma_{sn4}. \tag{22g–i}$$

As the eccentric distance ε approaches zero, $J_m(\alpha_{sn}\varepsilon)$ and $I_m(\alpha_{sn}\varepsilon)$ of equation (22a–c) will be zero for $m \neq 0$ and $J_m(\alpha_{sn}\varepsilon) = I_m(\alpha_{sn}\varepsilon) = 1$ for $m = 0$. Therefore, when $\varepsilon = 0$, equation (22) for the eccentric arrangement of the shell obviously reduces equation (17) of the concentric case. The concentrically submerged shell will be a special case of the shell submerged eccentrically in a fluid-filled container.

When the hydrostatic pressure on the shell is neglected for simple formulation, the hydrodynamic pressure along the outer wetted shell surface can be given by

$$p(x, \theta, t) = \rho_o \omega^2 \phi(R, \theta, x) \exp(i\omega t). \tag{23}$$

Finally, the hydrodynamic force on the shell can be written as

$$\frac{R^2 p(x, \theta, t)}{D} = \frac{\rho_o \omega^2 R^2}{D} \sum_{n=1}^{\infty} \left[\begin{array}{l} C_{on}\left\{\Gamma_{n1} J_n\left(\frac{\omega R}{c}\right) + \Gamma_{n2} Y_n\left(\frac{\omega R}{c}\right)\right\} \\ + \sum_{s=1}^{\infty} C_{sn}\{\Gamma_{sn3} I_n(\alpha_{sn}R) + \Gamma_{sn5} K_n(\alpha_{sn}R)\} \end{array} \right] \exp(i\omega t)$$

$$\text{for } \frac{s\pi}{L} \geqslant \frac{\omega}{c}, \tag{24a}$$

$$\frac{R^2 p(x,\theta,t)}{D} = \frac{\rho_o \omega^2 R^2}{D} \sum_{n=1}^{\infty} \left[\begin{array}{l} C_{on}\left\{ \Gamma_{n1} \mathrm{J}_n\left(\frac{\omega R}{c}\right) + \Gamma_{n2} \mathrm{Y}_n\left(\frac{\omega R}{c}\right)\right\} \\ + \sum_{s=1}^{\infty} C_{sn}\{\Gamma_{sn4} \mathrm{J}_n(\alpha_{sn} R) + \Gamma_{sn6} \mathrm{Y}_n(\alpha_{sn} R)\} \end{array} \right] \exp(\mathrm{i}\omega t)$$

$$\text{for } \frac{s\pi}{L} < \frac{\omega}{c}. \tag{24b}$$

2.6. GENERAL FORMULATION

The dynamic displacements and their derivatives can be represented by a Fourier sine and cosine series in an open range of $0 < x < L$ with the end values using the finite Fourier transformation [14]. Substitution of the displacements and their derivatives into the governing Sanders' shell equation (1a–c) leads to an explicit relation for C_{on} and a set of equations for A_{sn}, B_{sn}, C_{sn}, as follows:

$$\begin{bmatrix} B_{on} \\ C_{on} \end{bmatrix} = \boldsymbol{y}_1[u_o + u_l] + \boldsymbol{y}_2[v_o + v_l] + \boldsymbol{y}_3[\tilde{w}_o + \tilde{w}_l] + \boldsymbol{y}_4[\tilde{\tilde{w}}_o + \tilde{\tilde{w}}_l], \tag{25}$$

$$\begin{bmatrix} A_{sn} \\ B_{sn} \\ C_{sn} \end{bmatrix} = \boldsymbol{y}_5[u_o + (-1)^m u_l] + \boldsymbol{y}_6[v_o + (-1)^m v_l] + \boldsymbol{y}_7[\tilde{w}_o + (-1)^m \tilde{w}_l]$$

$$+ \boldsymbol{y}_8[\tilde{\tilde{w}}_o + (-1)^m \tilde{\tilde{w}}_l], \tag{26}$$

where the end values u_o, u_l, v_o, v_l, $\tilde{w}_o$, $\tilde{w}_l$, $\tilde{\tilde{w}}_o$, and $\tilde{\tilde{w}}_l$ in equations (25) and (26) are defined in reference [13]. The matrix $\boldsymbol{y}_1, \boldsymbol{y}_2, \ldots, \boldsymbol{y}_8$ are the derived column matrices. The equivalent hydrodynamic mass effect on the shell is included in the coefficient. The forces $N_{x\theta}$ and Q_x at the ends of the shells can be written as a combination of some boundary values of displacement and their derivatives using equation (4). The boundary values of displacement and their derivatives, v_o, v_l, $\tilde{\tilde{w}}_0$, and $\tilde{\tilde{w}}_l$ can be transformed into a combination of the boundary values of u, $\tilde{w}$, $N_{x\theta}$ and Q_x by equation (4), as written in the form

$$v_o = g_1 u_o + g_2 \tilde{w}_o + g_3 N^o_{x\theta}, \tag{27a}$$

$$v_l = g_1 u_l + g_2 \tilde{w}_l + g_3 N^l_{x\theta}, \tag{27b}$$

$$\tilde{\tilde{w}}_o = g_4 u_o + g_5 \tilde{w}_o + g_6 N^o_{x\theta} + g_7 Q^o_x, \tag{27c}$$

$$\tilde{\tilde{w}}_l = g_4 u_l + g_5 \tilde{w}_l + g_6 N^l_{x\theta} + g_7 Q^l_x, \tag{27d}$$

where the end values of the forces are defined in reference [13] and g_k ($k = 1, 2, \ldots, 7$) can be derived. Substitution of equation (27) into equations (25) and (26) gives

$$\begin{bmatrix} B_{on} \\ C_{on} \end{bmatrix} = z_1[u_o + u_l] + z_2[\tilde{w}_o + \tilde{w}_l] + z_3[N^o_{x\theta} + N^l_{x\theta}] + z_4[Q^o_x + Q^l_x], \quad (28a)$$

$$\begin{bmatrix} A_{sn} \\ B_{sn} \\ C_{sn} \end{bmatrix} = [\Lambda_{ik}] \begin{bmatrix} u_o + (-1)^m u_l \\ \tilde{w}_o + (-1)^m \tilde{w}_l \\ N^o_{x\theta} + (-1)^m N^l_{x\theta} \\ Q^o_x + (-1)^m Q^l_x \end{bmatrix}, \quad (28b)$$

where z_k ($k = 1, 2, 3, 4$) in equation (28a) are the derived coefficient matrices, and $[\Lambda_{ik}]$ ($i = 1, 2, 3$; $k = 1, 2, 3, 4$) in equation (28b) is the 4×3 derived coefficient matrix. Eventually, all Fourier coefficients A_{sn}, B_{sn} and C_{sn} are rearranged with a combination of the end point values, as shown in equation (28b).

The geometric boundary conditions that must be satisfied are associated with the dynamic displacement v and w as described in equation (3). Hence it follows that

$$v(0) = \sum_{n=1}^{\infty} \left[B_{on} + \sum_{s=1}^{\infty} B_{sn} \right] = 0, \quad v(L) = \sum_{n=1}^{\infty} \left[B_{on} + \sum_{s=1}^{\infty} B_{sn}(-1)^m \right] = 0, \quad (29a, b)$$

$$w(0) = \sum_{n=1}^{\infty} \left[C_{on} + \sum_{s=1}^{\infty} C_{sn} \right] = 0, \quad w(L) = \sum_{n=1}^{\infty} \left[B_{on} + \sum_{s=1}^{\infty} B_{sn}(-1)^m \right] = 0. \quad (29c, d)$$

Substitution of equation (28) for the coefficients B_{on}, C_{on}, A_{sn}, B_{sn}, and C_{sn} into the four constraint conditions that come from the geometric boundary condition, written as equation (29), leads to a homogeneous matrix equation by omitting the details:

$$\begin{bmatrix} e_{11} & e_{12} & e_{13} & e_{14} & e_{15} & e_{16} & e_{17} & e_{18} \\ e_{21} & e_{22} & e_{23} & e_{24} & e_{25} & e_{26} & e_{27} & e_{28} \\ e_{31} & e_{32} & e_{33} & e_{34} & e_{35} & e_{36} & e_{37} & e_{38} \\ e_{41} & e_{42} & e_{43} & e_{44} & e_{45} & e_{46} & e_{47} & e_{48} \end{bmatrix} \begin{Bmatrix} u_o \\ u_l \\ \tilde{w}_o \\ \tilde{w}_l \\ N^o_{x\theta} \\ N^l_{x\theta} \\ Q^o_x \\ Q^l_x \end{Bmatrix} = \{0\}. \quad (30)$$

The elements of the matrix, e_{ik} ($i = 1, 2, 3, 4$, $k = 1, 2, \ldots, 8$) can be obtained from equation (29). However, when the cylindrical shell is clamped at both support ends,

the associated boundary condition is

$$u = v = w = w_{,x} = 0 \quad \text{at } x = 0 \text{ and } L. \tag{31}$$

Among these boundary conditions, the two geometric boundary conditions $u = 0$ and $\tilde{w}_o = 0$ at $x = 0$ and $x = L$ are not automatically satisfied by equation (6), the modal functions set. Therefore the first, second, third, and fourth rows of the matrix in equation (30) are enforced and the terms associated with u_o, u_l, $\tilde{w}_o$, and $\tilde{w}_l$ are released. The 4×4 frequency determinant is obtained from equations (30) and (31) by retaining the rows and columns associated with $N^o_{x\theta}$, $N^l_{x\theta}$, Q^o_x, and Q^l_x. For the clamped boundary condition, the coupled natural frequencies are numerically obtained from the frequency determinant:

$$\begin{vmatrix} e_{15} & e_{16} & e_{17} & e_{18} \\ e_{25} & e_{26} & e_{27} & e_{28} \\ e_{35} & e_{36} & e_{37} & e_{38} \\ e_{45} & e_{46} & e_{47} & e_{48} \end{vmatrix} = 0. \tag{32}$$

3. EXAMPLE AND DISCUSSION

3.1. VERIFICATION OF ANALYTICAL METHOD

On the basis of the preceding analysis, the frequency determinant is numerically solved for the clamped boundary condition in order to find the natural frequencies of the circular cylindrical shell concentrically or eccentrically submerged in a fluid-filled cylindrical container. The fluid-filled annular gap distance and the eccentricity to the container affect the motion of the cylindrical shell. In order to check the validity and accuracy of the results from the theoretical study and compare them with the FEM result, computation is carried out for the fluid-coupled system. The cylindrical shell has a mean radius of 100 mm, a length of 300 mm, and a wall thickness of 2 mm. The outer cylindrical container has an inner radius of 110 mm with the same length for Case 1 and it has 130 mm of inner radius with the same length for Case 2. The physical properties of the shell material are as follows: Young's modulus = 69·0 GPa, the Poisson ratio = 0·3, and mass density = 2700 kg/m^3. Water is used as the containing fluid with a density of 1000 kg/m^3. The sound speed in water, 1483 m/s, is equivalent to the bulk modulus of elasticity, 2·2 GPa. The clamped boundary condition at both ends of the shell is considered.

The frequency equation derived in the preceding section involves the double infinite series of algebraic terms. Before exploring the analytical method for obtaining the natural frequencies of the fluid-coupled shell, it is necessary to conduct convergence studies and establish the number of terms required in the series expansions involved. In the numerical calculation, the Fourier expansion terms s is set at 80, which gives an exact enough solution by convergence. Additionally, the Bassel expansion term m is included in the numerical calculation for the case of eccentrically submerged shell. The expansion term m is set at 50,

which also gives a converged solution. Finite element analyses, using a commercial computer code ANSYS (version 5·2), are performed to verify the theoretical results for the concentrically submerged shell. The FEM results are used as the baseline data. In the finite-element analysis, two-dimensional axisymmetric models are constructed with axisymmetric two-dimensional fluid elements (FLUID81) and axisymmetric shell elements (SHELL61). The fluid region is divided into a number of identical fluid elements with four nodes. We model the circular cylindrical shell as deformable shell elements with two nodes. The fluid boundary conditions at the top and bottom of the tank are zero displacement and rotations. The nodes connected entirely by the fluid elements are free to move arbitrarily in three-dimensional space, with the exception of those restricted to motion in the bottom and top surfaces of the fluid cavity. The radial velocities of the fluid nodes along the wetted shell surfaces coincide with the corresponding velocities of the shells. The FEM model has 320 (radially $8 \times$ axially 40) fluid elements and 40 shell elements.

Table 1 will make it easier to check the accuracy of the frequencies and compare the theoretical frequencies with the corresponding FEM ones for the concentrically submerged shell. The discrepancy in the table is defined as

$$Discrepancy\ (\%) = \frac{Theoretical\ \ frequency - FEM\ \ frequency}{FEM\ \ frequency} \times 100. \tag{33}$$

The largest discrepancies between the theoretical and FEM results are 1·79% for Case 1 when $n = 1$, and $m' = 4$ and 2·53% for Case 2 when $n = 2$ and $m' = 3$. The discrepancies defined by equation (33), for the cases, are always less than 3% in the range of $n = 1$–8 and $m' = 1$–4. As the coarse mesh of the FEM model changes to the fine mesh, all natural frequencies may converge to the theoretical results. As can be seen, the present results for the concentrically submerged shell agree quite well with the FEM solution. Unfortunately, the verification for the eccentrically submerged case is not performed yet, because the finite-element analyses for the eccentric cases should be carried out using the three-dimensional model instead of the two-dimensional axisymmetric model. The three-dimensional model for the eccentrically submerged case requires a large number of elements and complicated boundary conditions along the wetted surfaces.

3.2. EFFECT OF RADIUS RATIO

First of all, in order to see the distance effect of surrounding annular fluid gap, the radius ratio is defined as

$$\delta = \left(\frac{R_0}{R}\right), \quad 1 < \delta < \infty. \tag{34}$$

when $R_0 \gg R$, δ approaches ∞. It obviously corresponds to the case of the shell submerged in an infinite fluid. On the contrary, as R_0 approaches R, the radius

TABLE 1

Comparison of FEM and theoretical coupled natural frequencies (Hz) for a cylindrical shell concentrically submerged in a fluid-filled rigid container

Mode		Coupled natural frequency (Hz)					
		Case 1 ($R_o = 0{\cdot}110$ m)			Case 2 ($R_o = 0{\cdot}130$ m)		
n	m'	FEM	Theory	Discrepancy (%)	FEM	Theory	Discrepancy (%)
1	1	334·1	333·7	− 0·12	536·4	532·7	− 0·69
	2	750·0	744·5	− 0·73	1219·1	1195·2	− 1·96
	3	1288·0	1271·2	− 1·30	2024·2	1974·6	− 2·45
	4	1893·9	1860·0	− 1·79	2802·5	2743·6	− 2·10
2	1	342·7	342·9	0·06	534·6	534·5	− 0·02
	2	756·8	755·3	− 0·20	1169·3	1162·7	− 0·56
	3	1263·2	1253·3	− 0·78	1897·0	1872·1	− 1·31
	4	1822·1	1795·3	− 1·44	2606·3	2545·1	− 2·35
3	1	316·5	316·5	0·00	468·3	468·5	0·04
	2	700·6	699·8	− 0·11	1022·0	1020·5	− 0·15
	3	118·8	1183·0	− 0·49	1689·7	1679·7	− 0·59
	4	1733·7	1715·0	− 1·08	2370·5	2343·8	− 1·13
4	1	337·7	337·4	− 0·09	471·3	471·4	0·02
	2	668·7	667·6	− 0·16	920·0	919·3	− 0·08
	3	1120·9	1116·1	− 0·43	1507·6	1502·5	− 0·34
	4	1647·5	1632·8	− 0·89	2148·2	2131·9	− 0·76
5	1	463·0	462·6	− 0·09	611·1	611·5	0·07
	2	719·8	718·2	− 0·22	938·0	937·4	− 0·06
	3	1120·4	1115·4	− 0·45	1432·5	1428·7	− 0·27
	4	1617·1	1603·7	− 0·83	2017·1	2005·2	− 0·59
6	1	700·2	699·6	− 0·09	878·9	879·9	0·11
	2	894·5	892·5	− 0·22	1111·2	1110·9	− 0·03
	3	1234·6	1229·0	− 0·45	1510·2	1506·9	− 0·22
	4	1690·5	1676·9	− 0·80	2028·1	2017·9	− 0·50

ratio δ will come near unity and the fluid annular gap formed by a shell and a rigid container is relatively narrow. One of the best ways to estimate the hydrodynamic effects on free vibration of a fluid-coupled structure is to obtain the non-dimensional normalized natural frequencies as described in the previous study [16]. The normalized natural frequency behaviour of the inner shell depending on water annular gap distances are illustrated in Figures 2–5, where the normalized natural frequency is defined as the fluid-coupled natural frequency divided by the natural frequency in vacuum for the specific corresponding mode. The normalized natural frequencies for the axial mode number $m' = 1$ are plotted in Figure 2 as a function of the circumferential mode number n in the cases of $\delta = 1{\cdot}1, 1{\cdot}2, 1{\cdot}3, 1{\cdot}5$, and $2{\cdot}0$. This figure shows that the natural frequency of the shell can be reduced by

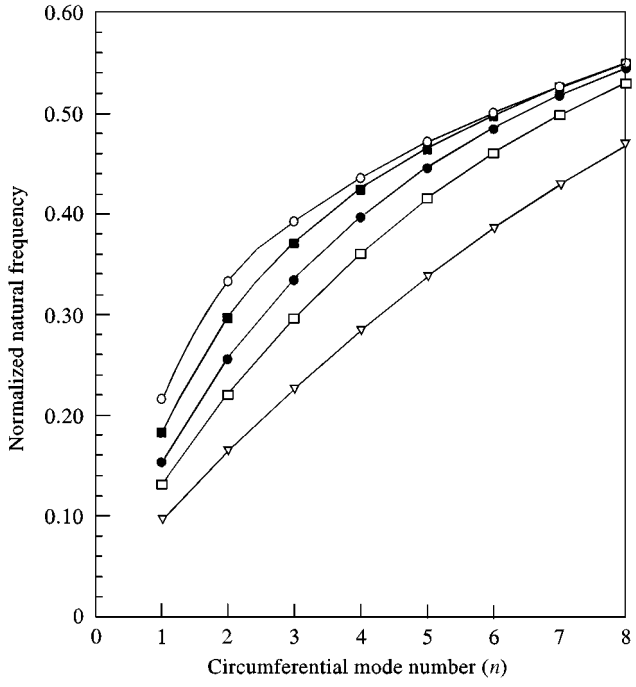

Figure 2. Normalized natural frequencies of a circular cylindrical shell concentrically submerged in a fluid-filled rigid container for $m' = 1$ (—▽—, $\delta = 1{\cdot}1$; —□—, $\delta = 1{\cdot}2$; —●—, $\delta = 1{\cdot}3$; —■—, $\delta = 1{\cdot}5$; —○—, $\delta = 2{\cdot}0$

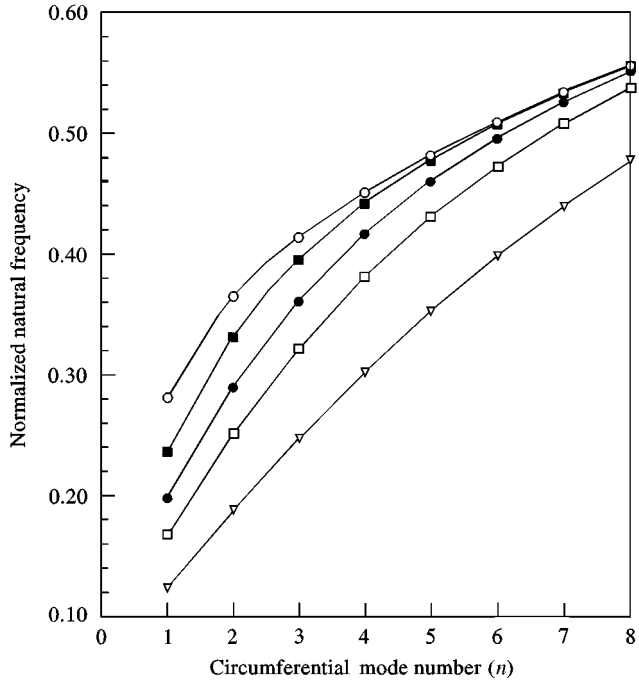

Figure 3. Normalized natural frequencies of a circular cylindrical shell concentrically submerged in a fluid-filled rigid container for $m' = 2$. Key as for Figure 2.

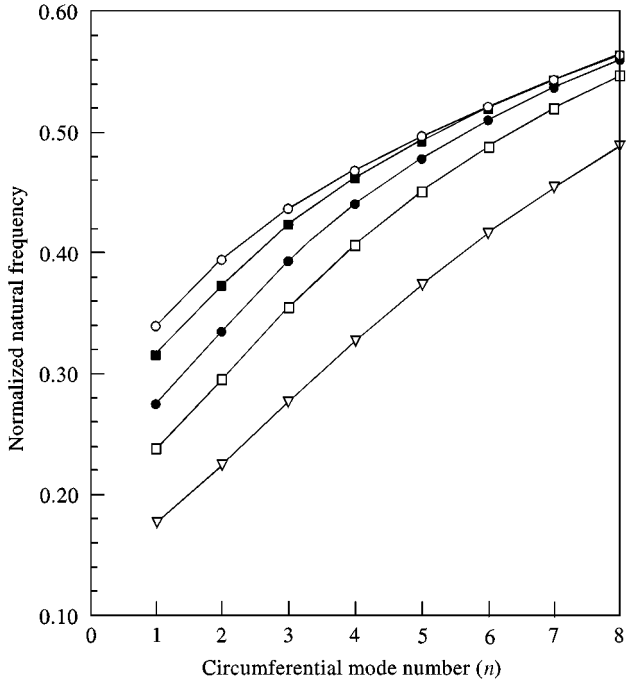

Figure 4. Normalized natural frequencies of a circular cylindrical shell concentrically submerged in a fluid-filled rigid container for $m' = 3$. Key as for Figure 2.

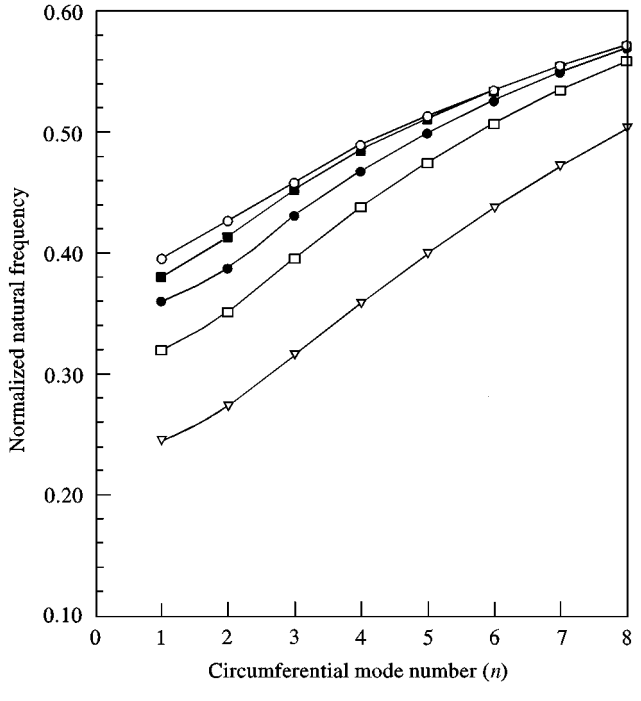

Figure 5. Normalized natural frequencies of a circular cylindrical shell concentrically submerged in a fluid-filled rigid container for $m' = 4$. Key as for Figure 2.

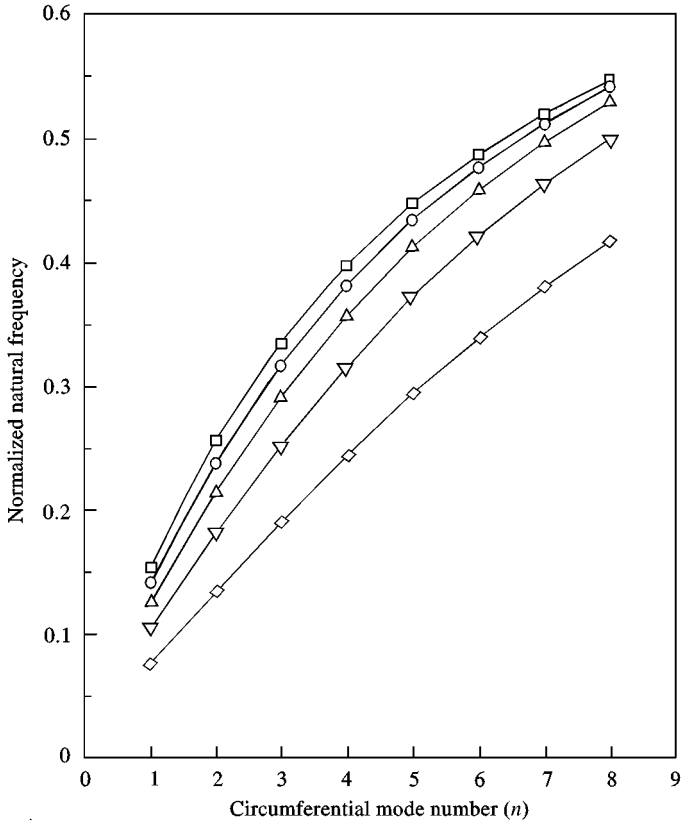

Figure 6. Effects of eccentricity on the normalized natural frequencies of a circular cylindrical shell eccentrically submerged in a fluid-filled rigid container for $m' = 1$ and $\delta = 1{\cdot}3$ (—□—, $\sigma = 0{\cdot}0$; —○—, $\sigma = 0{\cdot}2$; —△—, $\delta = 0{\cdot}4$; —▽—, $\delta = 0{\cdot}6$; —◇—, $\sigma = 0{\cdot}8$).

about 90% by coming into contact with water for $m' = 1$, $n = 1$ and $\delta = 1{\cdot}1$. For $m' = 2$, 3 and 4, similar figures are illustrated in Figures 3, 4 and 5 respectively. As one can see, the normalized natural frequencies are always less than unity due to the hydrodynamic mass (or the added mass) of fluid. When the circumferential mode number n increases, the normalized natural frequencies monotonically increase regardless of the axial mode, m', in the range of $1 \leqslant n \leqslant 8$ due to the *separation effect* explained by Jeong and Lee [16]. Judging from Figures 2–5, it is also clear that for the same reason the normalized natural frequencies also increase with an increase in the axial mode number. If the radius ratio δ approaches unity, the normalized natural frequencies decrease drastically because the narrow annular gap produces a great hydrodynamic mass due to a lengthened moving length of fluid. That is to say, the narrow annular gap works as a one directional channel carrying fluid during vibration, which produces an increased hydrodynamic mass, and eventually reduces the natural frequencies of the shell. On the contrary, as the fluid annular gap distance increases, the moving length of fluid during vibration is relatively shortened and eventually the hydrodynamic mass is also reduced. When the radius ratio $\delta > 2{\cdot}0$ and the circumferential mode number $n > 5$, the results are

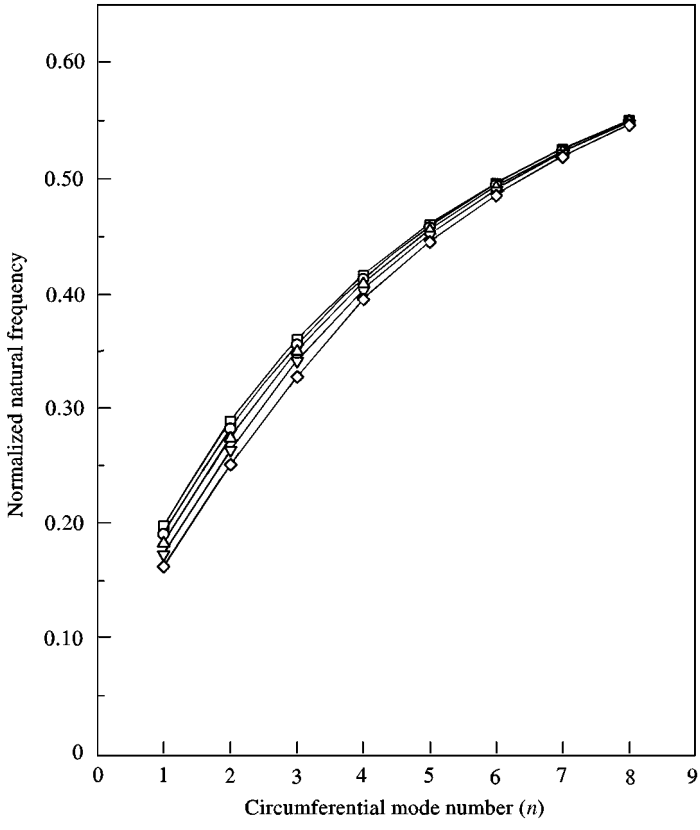

Figure 7. Effects of eccentricity on the normalized natural frequencies of a circular cylindrical shell eccentrically submerged in a fluid-filled rigid container for $m' = 2$ and $\delta = 1{\cdot}3$. Key as for Figure 6.

not different from the case when it is surrounded with an infinite fluid. This shows the case of the radius ratio $\delta > 2{\cdot}0$ with a circumferential higher mode that can be treated as a shell submerged in an infinite fluid. However, the assumption that a cylindrical shell is submerged in an infinite fluid, in order to get the natural frequencies of a concentrically submerged shell in a fluid-filled container with a relatively wide annular gap, may lead to overestimation of the natural frequencies for lower circumferential modes.

3.3. EFFECT OF ECCENTRICITY

The effect of eccentricity on the natural frequency is investigated in this section. The eccentricity of the shell to the container, σ, is defined as

$$\sigma = \left(\frac{\varepsilon}{R_0 - R} \right), \quad 0 \leqslant \sigma < 1. \tag{35}$$

As an extreme case, when the two origins "O" and "O′" in Figure 1 get close to each other, the eccentric distance ε will be zero. Hence, the eccentricity $\sigma = 0$

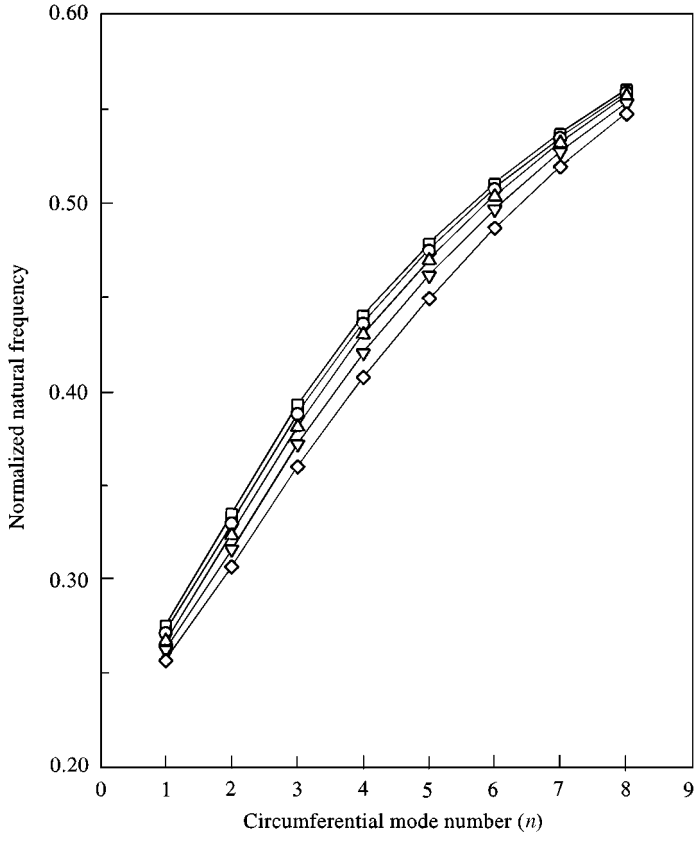

Figure 8. Effects of eccentricity on the normalized natural frequencies of a circular cylindrical shell eccentrically submerged in a fluid-filled rigid container for $m' = 3$ and $\delta = 1{\cdot}3$. Key as for Figure 6.

corresponds to the case of the concentrically submerged shell. The effects of the eccentricity on natural frequencies are illustrated in Figures 6–10. Figure 6 shows the eccentricity effect of the shell on the normalized natural frequencies for $m' = 1$. In the figure, the normalized natural frequencies are found to gradually increase with an increase of the circumferential mode number for any eccentricity. Additionally, the figure shows that the normalized natural frequencies decrease with an increase of the eccentricity. Especially, as the eccentricity approaches unity, the drop of normalized natural frequencies is accelerated. However, for axial mode number $m' = 2$, and 3, the effect of eccentricity on the normalized natural frequencies appear relatively small as shown in Figures 7 and 8. One reason can be that the tangential movement of fluid along the annular fluid gap for $m' = 1$ is changed to the combined movement to the tangential and vertical directions for $m' > 1$. The change of fluid movement direction during vibration of the shell makes the moving length of fluid relatively shorter, which contributes the reduction of hydrodynamic mass along with the reduction in the eccentricity effect for $m' > 1$. Therefore, the effect of eccentricity appears to be most pronounced for axial mode number $m' = 1$. Figures 9 and 10 illustrate the ratios of the natural frequencies for

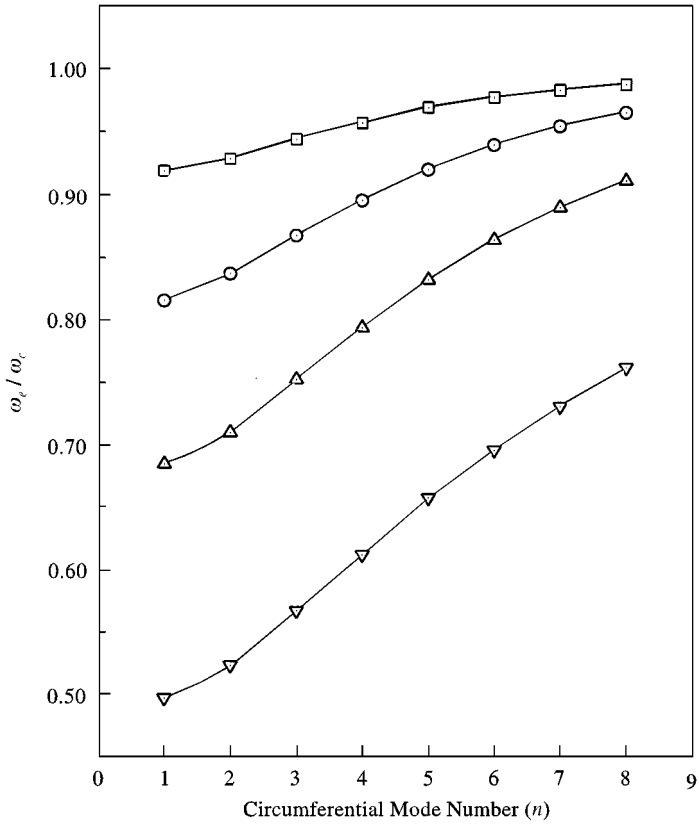

Figure 9. Natural frequencies ratios of the eccentrically submerged shell to the concentrically submerged case for $m' = 1$ and $\delta = 1{\cdot}3$ (—□—, $\sigma = 0{\cdot}2$; —○—, $\sigma = 0{\cdot}4$; —△—, $\sigma = 0{\cdot}6$; —▽—, $\sigma = 0{\cdot}8$).

the eccentrically submerged case to those of the concentrically submerged case. In the figures, ω_c and ω_e represent the natural frequencies for the concentrically submerged case and the eccentrically submerged case respectively. Figure 9 also shows that the natural frequency can be reduced by about 50% due to the eccentricity only when $m' = 1$, $n = 1$, $\delta = 1{\cdot}3$ and $\sigma = 0{\cdot}8$. It is also found that the eccentricity effect on the natural frequencies of the shell is dominant for lower vertical and circumferential modes.

4. CONCLUSIONS

A theoretical study on the natural frequencies of a circular cylindrical shell concentrically or eccentrically submerged in a fluid-filled rigid cylindrical container is conducted. In order to consider an eccentricity between the axes of the shell and the container, Graf's additional theorem and Beltrami's theorem are used for the translated forms of the Bassel functions in the shifted co-ordinate system. The proposed analytical method for the concentrically submerged shell is verified by the finite-element method, the results of which show excellent agreement. In order to

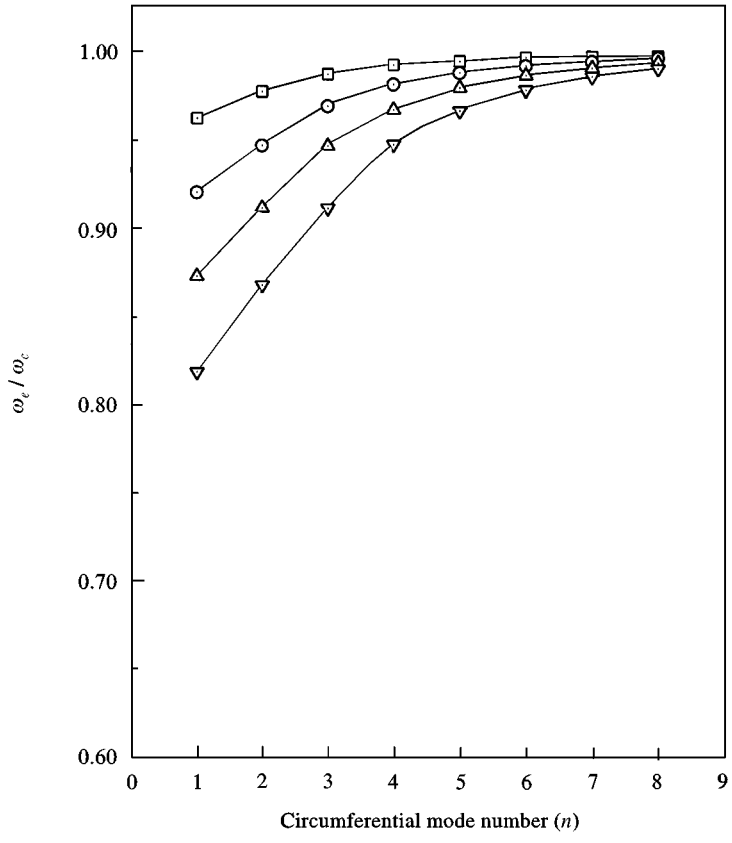

Figure 10. Natural frequencies ratios of the eccentrically submerged shell to the concentrically submerged case for $m' = 2$ and $\delta = 1{\cdot}3$. Key as for Figure 9.

evaluate the dynamic characteristics of the fluid-coupled system, the effects of annular fluid gap distance and eccentricity of the shell to the container on the natural frequencies are investigated. It is found that an increase of the annular gap between the shell and rigid container produces an increase of the natural frequencies of the shell for all circumferential and axial modes. The eccentricity of the shell tends to reduce the natural frequencies for all axial and circumferential mode numbers. The eccentricity effect on the natural frequencies is found to be especially dominant for axial mode number $m' = 1$.

REFERENCES

1. D. KRAJCINOVIC 1974 *Nuclear Engineering and Design* **30**, 242–248. Vibration of two coaxial cylindrical shells containing fluids.
2. S. S. CHEN and G. S. ROSENBERG 1975 *Nuclear Engineering and Design* **32**, 302–310. Dynamics of a coupled shell-fluid system.
3. M. K. AU-YANG 1975, *NPGD-TM*-320, Babcock & Wilcox. Free vibration of fluid-coupled coaxial cylinders of different lengths.

4. R. Endo and N. Tosaka 1989 *JSME International Journal* (Series I) **32**, 217–221. Free vibration analysis of coupled external fluid-elastic cylindrical shell-internal fluid system.
5. J. Tani, K. Otomo, T. Sakai and M. Chiba 1989 *Sloshing and Fluid–Structure Vibration*-1989. PVP **157**, 29–34. Hydroelastic vibration of partially fluid-filled coaxial cylindrical shells.
6. S. Yoshikawa, E. G. Williams and K. B. Washburn 1994 *Journal of the Acoustical Society of America* **95**, 3273–3286. Vibration of two concentric submerged cylindrical shells coupled by the entrained fluid.
7. M. Chiba 1995 *Journal of the Acoustical Society of America* **95**, 2238–2248. Free vibration of a clamped-free circular cylindrical shell partially submerged in a liquid.
8. K. H. Jeong and S. C. Lee 1996 *Computers & Structures* **58**, 937–946. Fourier series expansion method for free vibration analysis of either a partially fluid-filled or a partially fluid-surrounded circular cylindrical shell.
9. M. Chiba and H. Osumi 1998 *Journal of Sound and Vibration* **209**, 771–796. Free vibration and buckling of a partially submerged clamped cylindrical tank under compression.
10. K. H. Jeong 1998 *Journal of Sound and Vibration* **215**, 105–124. Natural frequencies and mode shapes of two coaxial cylindrical shells coupled with bounded compressible fluid.
11. E. B. Danila, J. M. Conoir and J. L. Izbicki 1995 *Journal of the Acoustical Society of America* **98**, 3326–3342. The generalized Debye series expansion: treatment of the concentric and non-concentric cylindrical fluid–fluid interfaces.
12. H. Chung 1981 *Journal of Sound and Vibration* **74**, 331–350. Free vibration analysis of circular cylindrical shells.
13. K. H. Jeong and K. J. Kim 1998 *Journal of Sound and Vibration* **217**, 197–221. Free vibration of a circular cylindrical shell filled with bounded compressible fluid.
14. I. N. Sneddon 1951 *Fourier Transforms* 72–76, New York: McGraw-Hill.
15. G. N. Watson 1980 *A Treatise on the Theory of Bassel Functions*, 360–361. Cambridge: Cambridge University Press, second edition.
16. K. H. Jeong and S. C. Lee 1998 *Computers & Structures* **66**, 173–185. Hydroelastic vibration of a liquid-filled circular cylindrical shell.

APPENDIX: NOMENCLATURE

A_{sn}	Fourier coefficient related to modal function in the axial direction
a	radial co-ordinate for shifted co-ordinate system with origin "O′"
B	bulk modulus of elasticity of the fluid
B_{on}, B_{sn}	Fourier coefficients related to modal function in the azimuthal direction
C_{on}, C_{sn}	Fourier coefficients related to modal function in the radial direction
c	speed of sound in the fluid medium
D	$= Eh/(1-\mu^2)$
D_{on}, D_{sn}	Fourier coefficients related to fluid motion
E	Young's modulus of the shell
e_{ik}	derived coefficients in equation (30), where $i = 1, 2, \ldots, 4$ and $k = 1, 2, \ldots, 8$
F_{on}, F_{sn}	Fourier coefficients related to fluid motion
$f(x)$	spacial velocity potential in the axial direction defined in equation (8)
g_k	derived coefficients in equation (27), where $k = 1, 2, \ldots, 7$
i	imaginary unit
h	thickness of the cylindrical shell
K	$= Eh^3/12(1-\mu^2)$
k	$= h^2/12R^2$
m	series expansion terms for Graf's additional theorem and Beltrami's theorem
m'	axial mode number

M_x bending moment per unit length
$N_{x\theta}$ effective membrane shear force per unit length
N_x membrane tensile force per unit length
n circumferential mode number
L height of the shell
p hydrodynamic pressure on the shell
Q_x effective transverse shear force per unit length
R mean radius of the shell
R_o inner radius of the rigid container
r radial co-ordinate for the original co-ordinate system with origin "O"
s Fourier components in the axial direction
t time
u axial dynamic displacement of the shell
v tangential dynamic displacement of the shell
W_{n1}, W_{n2}, W_{n3} coefficients defined in equations (22a)–(22c)
w radial dynamic displacement of the shell
$\tilde{w}, \tilde{\tilde{w}}$ end values defined in reference [13]
x axial co-ordinate
$\boldsymbol{y}_j$ derived column matrices defined in equations (25) and (26), where $j = 1, 2, \ldots, 8$
z_k derived column matrices defined in equation (28a) where $k = 1, 2, \ldots, 4$
α_{sn} parameter defined in equation (11)
Γ_{n1}, Γ_{n2} coefficients defined in equations (22d) and (22e)
$\Gamma_{sn3}, \ldots, \Gamma_{sn6}$ coefficients defined in equations (22f)–(22i)
δ $= R_o/R$
ε eccentric distance between the central axes "O" and "O′"
γ^2 $= \rho R^2(1-\mu^2)/E$
η velocity potential function of r and θ
θ tangentical co-ordinate for original co-ordinate system with origin "O"
$[\Lambda_{ik}]$ derived matrix defined in equation (28b), where $i = 1, 2, 3$ and $k = 1, 2, 3, 4$
μ Poisson ratio of the shell
ρ density of the cylindrical shell
ρ_o density of the fluid
σ $= \varepsilon/(R_o - R)$
Φ general velocity potential function of r, θ, x and t
ϕ spatial velocity potential function of r, θ and x
ψ tangential co-ordinate for shifted co-ordinate system with origin "O′"
ω coupled natural frequency
ω_c coupled natural frequency of concentrically submerged shell
ω_e coupled natural frequency of eccentrically submerged shell

Indices value at $x = 0$
value at $x = L$